Accepted to Ap.J.
Preprint typeset using LaTeX style emulateapj v. 6/22/04

A NEW MECHANISM FOR CORE-COLLAPSE SUPERNOVA EXPLOSIONS

A. Burrows[1], E. Livne[2], L. Dessart[1], C.D. Ott[3], J. Murphy[1]

Accepted to Ap.J.

ABSTRACT

In this paper, we present a new mechanism for core-collapse supernova explosions that relies upon acoustic power generated in the inner core as the driver. In our simulation using an 11-$M_\odot$ progenitor, an advective-acoustic oscillation à la Foglizzo with a period of $\sim$25$-$30 milliseconds (ms) arises $\sim$200 ms after bounce. Its growth saturates due to the generation of secondary shocks, and kinks in the resulting shock structure funnel and regulate subsequent accretion onto the inner core. However, this instability is not the primary agent of explosion. Rather, it is the acoustic power generated early on in the inner turbulent region stirred by the accretion plumes, and most importantly, but later on, by the excitation and sonic damping of core g-mode oscillations. An $\ell = 1$ mode with a period of $\sim$3 ms grows at late times to be prominent around $\sim$500 ms after bounce. The accreting protoneutron star is a self-excited oscillator, "tuned" to the most easily excited core g-mode. The associated acoustic power seen in our 11-$M_\odot$ simulation is sufficient to drive the explosion >550 milliseconds after bounce. The angular distribution of the emitted sound is fundamentally aspherical. The sound pulses radiated from the core steepen into shock waves that merge as they propagate into the outer mantle and deposit their energy and momentum with high efficiency. The ultimate source of the acoustic power is the gravitational energy of infall and the core oscillation acts like a transducer to convert this accretion energy into sound. An advantage of the acoustic mechanism is that acoustic power does not abate until accretion subsides, so that it is available as long as it may be needed to explode the star. This suggests a natural means by which the supernova is self-regulating.

Subject headings: supernovae, neutrinos, multi-dimensional radiation hydrodynamics, stellar pulsations

1. INTRODUCTION

The essence of the mechanism of core-collapse supernovae must be the conversion of a fraction of the reservoir of gravitational energy into the kinetic and internal energy of the exploding mantle of the Chandrasekhar core whose instability inaugurates core collapse. A protoneutron star (PNS) is left which evolves into a cold neutron star most of the time, or, rarely, is the intermediate state along the way to the formation of a stellar-mass black hole through the general-relativistic instability [4]. Due predominantly to prodigious neutrino radiation (losses) over hundreds of milliseconds to seconds, the PNS becomes more and more bound, on its way to achieving a total binding energy near $\sim 3\times10^{53}$ ergs, a mass-energy equivalent of $\sim$0.15 $M_\odot$. This is far in excess of the $\sim 10^{51}$ ergs of the supernova explosion, so it has long been thought that 1) the mechanism of explosion is very inefficient, and 2) there is so much energy in the neutrino emissions that if only a small fraction were captured in the mantle it could be driven to explosion. The latter notion is the essence of the "neutrino-driven" mechanism, first adumbrated in its direct form by Colgate & White (1966) and Arnett (1966) and in its delayed form by Wilson (1985) and Bethe & Wilson (1985). However, using the best input physics and numerics, it has been shown that in spherical symmetry both the prompt and the delayed-revitalization neutrino heating mechanisms fail (Rampp & Janka 2000; Liebendörfer et al. 2001; Thompson, Burrows, & Pinto 2003). Moreover, the suggestion by Wilson (1985), Wilson & Mayle (1988,1993), and Mayle & Wilson (1988) that "neutron-finger" instabilities interior to or near the neutrinospheres can advect heat, and thereby boost the driving neutrino luminosities sufficiently to lead to pseudo-spherical explosions, has been dealt a severe blow by the more detailed analyses of Bruenn & Dineva (1996), Bruenn, Raley, & Mezzacappa (2004), and Dessart et al. (2005). Finally, through two decades of simulations, the idea that on dynamical times the bounce itself could, by direct piston action on the outer mantle, launch a successful shock wave that does not stall into accretion has been refuted. Due to significant shock breakout neutrino losses and nuclear photodissociation, the shock must stall.

Out of the ashes of the one-dimensional (1D), spherical models was born the idea that multi-dimensional neutrino-driven convection could increase the efficiency of neutrino heating behind the stalled shock and lead to a delayed explosion (Herant et al. 1994; Burrows, Hayes, & Fryxell 1995; Janka & Müller 1996; Fryer & Warren 2002,2004). Such neutrino-driven convection arises naturally and does increase the radius of the stalled shock

[1] Department of Astronomy and Steward Observatory, The University of Arizona, Tucson, AZ 85721; burrows@as.arizona.edu,luc@as.arizona.edu,jmurphy@as.arizona.edu
[2] Racah Institute of Physics, The Hebrew University, Jerusalem, Israel; eli@frodo.fiz.huji.ac.il
[3] Max-Planck-Institut für Gravitationsphysik, Albert-Einstein-Institut, Golm/Potsdam, Germany; cott@aei.mpg.de

[4] Direct formation of a black hole from a quasi-degenerate Chandrasekhar core is not possible, since the inner homologous core whose bounce halts collapse is out of sonic contact with the outer mantle. The inner core has a mass of but 0.5-0.7 $M_\odot$; it is only after sufficient mass has accreted subsequent to bounce that the object might experience the general-relativistic instability (which acts on sub-millisecond timescales) leading to collapse to a black

the neutrinospheres where there is net neutrino energy deposition. This is the current paradigm and models that did not explode in 1D have indeed exploded in 2- and 3-D. However, all these previous successful explosions were obtained in the context of simplified or gray treatments of neutrino transport and it has long been suspected that more sophisticated, multi-group, multi-angle treatments of neutrinos in the multi-dimensional spatial context were needed. In fact, though implementing 2D neutrino transport in an approximate way, Rampp & Janka (2002) and Buras et al. (2003,2005) use 2D hydrodynamics and one of the best available multi-group co-moving-frame Boltzmann solvers and do not obtain explosions[5]. Despite incorporating the best input physics, and coming tantalizingly close to explosion, their simulations lead to fizzles, calling into question the neutrino-driven mechanism itself. Within 200-300 milliseconds of bounce, after growing out to 150-200 kilometers, their shocks recede and are declared to be unsuccessful.

If the energy transfer from the core to the mantle necessary to explode the star is by neither direct hydrodynamics nor neutrino heating, what is left? How do core-collapse supernovae explode? In this paper we propose a new alternative, the generation in the core and the propagation into the mantle of strong sound waves. Acoustic power is, potentially, an efficient means to transport energy and momentum into the outer mantle to drive the supernova explosion. Unlike neutrinos, sound is almost 100% absorbed in the matter, though some of the acoustic energy is reradiated by neutrinos. As sound pulses propagate outward down the density gradient they steepen into multiple shock waves that catch up to one another and merge; a shock wave is almost a perfect black-body absorber of sound. If sufficient sound is generated in the core, it would be a natural vehicle for the gravitational energy of infall to be transferred to the outer mantle and could be the key missing ingredient in the core-collapse explosion mechanism. Furthermore, periodic shocking due to multiple sound pulses can lead naturally to entropies in the debris of hundreds of units, just what is required for r-process nucleosynthesis (Woosley & Hoffman 1992; Woosley et al. 1994; Hoffman et al. 1996).

We believe we have identified a vigorous source for the necessary acoustic power: the excitation and oscillation of core pulsation modes in the deep interior of the PNS. Using the 2D radiation/hydrodynamic code VULCAN/2D we have discovered that turbulence and anisotropic accretion in the inner $40-100$ kilometers can excite and maintain vigorous core g-mode oscillations which decay by the radiation of sound. The inner core acts as a transducer for the conversion of accretion gravitational energy into acoustic power. The associated acoustic power seen in our simulations is sufficient to drive the explosion >550 milliseconds after bounce.

In §2, we summarize the input physics, computational capabilities, and numerical approaches incorporated into the current version of our radiation/hydrodynamics code VULCAN/2D. Then, in §3 we describe our baseline simulation results for the 11 $M_\odot$ progenitor star on which we focus. This section defines the various hydrodynamic stages and events and explores the important, but secondary, role of the advective/acoustic or "SASI" instability highlighted by Foglizzo and collaborators (Foglizzo 2000,2001; Foglizzo & Tagger (2002); Foglizzo, Galletti, & Ruffert 2005) and by Blondin, Mezzacappa, & DeMarino (2003). We also introduce the key role played at late times by acoustic power and the emergence of core oscillation modes and discuss some aspects of the components of the mechanism we envision. Then, in §4, we summarize the general advantages of acoustic driving, and follow this in §5 with an investigation into the excitation of core oscillation modes, the associated general physics, and their acoustic damping. After this, we summarize in §6 the emerging role of neutrinos as important, but secondary, players in the explosion mechanism we are presenting. Finally, in §7 we reiterate the central features of our new mechanism, explain why it was not discovered earlier, and speculate on what now needs to be done both to test our hypothesis and to further advance our understanding of this central problem in theoretical astrophysics.

2. COMPUTATIONAL APPROACH AND INPUT PHYSICS

The code VULCAN/2D uses the hydrodynamic approach described in Livne (1993), with the transport methods discussed in Livne et al. (2004) and Walder et al. (2005). It is a Newtonian, 2D, multi-group, multi-angle radiation/hydrodynamics code with an Arbitrary-Lagrangian-Eulerian (ALE) structure (with remap) and a Multi-Group, Flux-Limited Diffusion (MGFLD) variant. Velocity terms in the transport sector, such as Doppler shifts, are not included in the code, though advection is. Note that the velocity terms in Eulerian transport are different from the coresponding terms in the co-moving frame and that general statements about their relative importance are very frame-dependent[6]. We parallelize in energy groups using MPI and do not include redistribution by neutrino-electron scattering in the 2D code. Such redistribution and scattering are of modest import on infall, affecting the trapped electron fraction (Y_e) and entropy (S) by $\sim$10%, but are otherwise quite subdominate. At a neutrino energy of 10 MeV, the neutrino-electron scattering cross section is $\sim$100 times smaller than the dominant cross sections off nucleons. Thompson, Burrows, & Pinto (2003) have devised and implemented an explicit scheme to handle redistribution that adds only $\sim 10-15\%$ to the computational time and this approach will be incorporated in future versions of VULCAN/2D. Note that the attempt to handle the full energy/angle redistribution problem implicitly has resulted in codes that are thereby slower by many *factors* (not percent), severely inhibiting their use for explorations in supernova theory.

In this paper, due to its relative speed, we use the MGFLD implementation of VULCAN/2D. The flux limiter is a vector version of the one found in Bruenn (1985). The code can handle rotation, though the results reported here are for a non-rotating progenitor. In 2D, the calculations are axially/azimuthally symmetric, and we use cylindrical coordinates (r and z), but the grid points themselves can be placed at arbitrary positions. This allows us to employ a Cartesian grid at the center

[5] unless they drop their many velocity-dependent terms, some-

(inner ∼20 kilometers) and transition to a spherical grid further out. The grid resolution is essentially uniform everywhere within ∼20 km. A version of this grid structure is plotted in Ott et al. (2004). The Cartesian format in the interior allows us to avoid the severe Courant problems encountered in 2D by all other groups employing grid-based codes due to the inner angular Courant limit and, thereby, to perform the calculations in full 2D all the way to the center. In many simulations to date, the inner core was calculated in 1D and grafted onto an outer region that was handled in 2D (e.g., Burrows, Hayes, & Fryxell 1995; Swesty & Myra 2005ab), or was excised completely (e.g., Janka & Müller 1996; Blondin, Mezzacappa, & DeMarino 2003; Scheck et al. 2004). In others, the 2D simulation was done on a ∼90° wedge, with the inner 2 or 25 km done in 1D (Buras et al. 2005). The gray SPH simulations of Herant et al. (1994) and Fryer & Warren (2002,2004) are an exception. Originally, a major motivation for this global 2D feature was the self-consistent investigation of core translational motion and neutron star kicks. However, as we will see, freeing the core has other advantages.

To determine the gravitational potential field we use a finite-difference approach to solve the Poisson equation. In addition, we incorporate the gravitational force along the symmetry axis in an automatically momentum-conserving fashion by writing it in divergence form. VULCAN/2D has an option to move the grid after bounce to maintain the best zoning under the core, whether it moves or not, while at the same time tracking this core motion. This feature ensures that the highest resolution is placed under most of the mass. Outside of the Cartesian mesh, the baseline calculation employs 121 angular zones equally spaced over 180°, and logarithmically allocates 162 radial shells between ∼20 km and the outer radius at 3800 km[7].

We employ the equation of state (EOS) of Shen et al. (1998), since it correctly incorporates alpha particles and is easily extended to lower densities. The neutrino-matter interaction physics is taken from Thompson, Burrows, & Pinto (2003) and Burrows & Thompson (2004). The tables generated in $\mathrm{T}/\rho/\mathrm{Y}_e$/neutrino-species space incorporate all relevant scattering, absorption, and emission processes. We follow separately the electron neutrino (ν_e) and anti-electron neutrino ($\bar{\nu_e}$), but for computational efficiency we lump the four remaining known neutrinos into "ν_μ" bins in the standard fashion. Our baseline model has 16 energy groups for each species, distributed logarithmically from 1 to 200 MeV. More energy groups would be better. Due to extreme matter-suppression effects, we have not felt it necessary to incorporate the effects of neutrino oscillations (Strack & Burrows 2005).

The instabilities that develop in the early stages of the post-bounce phase are seeded by the slight perturbations introduced due to the non-orthogonal shape of the grid regions that effect the transition from the inner Cartesian grid to the outer spherical grid (see Fig. 4 in Ott et al. 2004) and by noise at the part in $\sim 10^6$ level in the EOS table interpolation. Since the resulting turbules execute more than twenty overturns during the initial phase of convective instability, and this convective phase reaches a quasi-steady state, the initial conditions and the initial perturbations are completely lost in subsequent evolution. The seeds for the later shock instability are the non-linear convective structures that arise in the first post-bounce tens of milliseconds. Beyond these, we introduce no artificial numerical perturbations.

[7] For future calculations, the outer boundary radius should prob-

3. SIMULATION RESULTS

To demonstrate and represent the various core-collapse and post-bounce phases we think are important, we focus in this paper exclusively on results using the 11-$\mathrm{M}_\odot$ progenitor without rotation from Woosley & Weaver (1995), with the zoning and physics packages referred to in §2. Progenitor dependences will be left to future work. The calculations were done from ∼200 millseconds before bounce to ∼660 milliseconds after bounce, significantly longer than most (though not all) multi-D simulations in the literature [8]. We have generated movies of the runs, which are available from the authors upon request. Here, we provide a sequence of stills depicting phenomena or transitions of relevance, along with analysis plots that help to clarify salient features.

Figures 1 through 3 are an evolutionary sequence of the entropy distribution for the core region 750 kilometers on a side, with velocity vectors superposed to map out the evolving and complicated flow fields. The sequence includes snapshots at times of 50, 150, 275, 310, 385, 420, 470, 515, 575, and 608 milliseconds after bounce. In the last two stills, the supernova has clearly started to explode.

In the sequences depicted in Figs. 1, 2, & 3, we don't show the collapse phase because it is canonical and spherical. At ∼50 ms after bounce the shock has stalled, is roughly spherical, and is at a spherical radius (R) of ∼115 km. Neutrino-driven convection has begun in the region ∼50 km wide interior to the shock wave. Despite the advection correction to the standard convective instability criterion pointed out by Foglizzo, Scheck, & Janka (2005), we find that standard neutrino-driven convection at this stage has not been suppressed, though there is evidence of a weak $\ell = 1$ pulsation similar to what has been identified by Foglizzo and collaborators and by Blondin, Mezzacappa, & DeMarino (2003) (Figs. 4 and 5). By ∼150 ms, the average shock radius has reached ∼150 km, and the convection is encompassing the region down to $R \sim 75$ km. In the full angular region of 180°, we see 5-6 dominant turbules (eddies) with angular scales of ∼30-35°. Near ∼200 ms, the average shock radius has receded back to ∼110 km (Figs. 4 and 5). If shock recession had been our criterion for failure, we might have stopped the calculation here. However, at around ∼200 ms, the shock is beginning to wobble up and down perceptibly in an $\ell = 1$ mode with a period near 25-30 ms and a $\Delta R/R$ near 25%. At ∼250 ms, the $\Delta R/R$ is approaching ∼50% and the up-down asymmetry is quite pronounced. The growth time for the shock anisotropy varies, but is near 50-100 ms. We identify this early quasi-periodic oscillation with the advective-acoustic instability and the "standing accretion shock instability" (SASI) suggested by Foglizzo (2001,2002), Foglizzo &

Tagger (2000), Foglizzo, Galletti, & Ruffert (2005), and by Blondin, Mezzacappa, & DeMarino (2003), referred to from now on as the "shock instability."

By ∼300-350 ms, $\Delta R/R$ has grown to a factor of two and the wobble is taking on a more vigorous character. However, by ∼275 ms it has clearly entered the nonlinear regime. In particular, when one side is executing its outward oscillation, the material in its outer extent reverses its flow direction out of phase with the material further in. The result is the generation, where these two regions collide, of a secondary shock wave; the flow now has nested shock waves. The creation of secondary shocks serves to saturate the amplitude of the shock oscillation, which nevertheless continues. Furthermore, the corrugation of the outer shock, where there is a kink in the shock normal, propagates in latitude in both hemispheres and collides at the poles, first at 0° then at 180°. In part, this shock focussing is an artifact of the 2D nature of the simulation, but similar effects are seen in 3D pure hydro simulations (J. Blondin, private communication) and are expected from generic considerations. Each time the shock kinks collide, entropy and pressure (p) are generated and this pressure pulse moves at the speed of sound to the opposite side. Importantly, at the shock intersection kinks, clearly seen in Figs. 1 and 2 at 310 and 385 ms, the accretion through the outer shock is channeled and penetrates in lower entropy streams into the interior and onto the core. This phenomenon was previously seen by, among others, Herant et al. (1994), Burrows, Hayes, & Fryxell (1995), Fryer & Warren (2002), Rampp & Janka (2002), Scheck et al. (2004), Janka et al. (2005ab), and Buras et al. (2005). Though $\Delta R/R$ can reach factors of 3 or greater, this ratio always eventually decreases, if temporarily, and stabilizes. The angle-averaged outer shock radius does not increase monotonically. For instance, though at ∼385 ms, one lobe of the outer shock reaches ∼400 km, as Fig. 2 indicates, at ∼420 ms the average radius has receded temporarily to ∼250 km. The 2D hydro calculations of Blondin, Mezzacappa, & DeMarino (2003) that identified this instability were done without neutrino physics, and with an artifical inner boundary; they were done without electron capture, neutrino heating, neutrino cooling, and the core. Nevertheless, with neutrino physics and the core fully included, we verify the existence of this shock instability, first promoted by Foglizzo (2000,2001).

However, we have discovered significant and important differences with the work of Blondin, Mezzacappa, & DeMarino (2003) and with the expectations from the work of Foglizzo and collaborators. First, the shock instability does not lead to an increase in the average shock radius in the first 150-200 ms after bounce. Due to electron capture at the shock and to the quasi-hydrostatic sinking of the inner core caused by steady neutronization and cooling, an "$\ell = 0$" component is not in evidence. Shock asphericities with some $\ell = 1$ component are generated, but mostly by the turbulent motions of neutrino-driven convection during this early phase. It is only after the core has settled, the electron capture rates at the shock have decreased due to the gradual decrease in the density of the accreted material, and there is no net energy loss behind the shock in the gain region that the advective-acoustic behavior identified by Foglizzo is tured in the calculations of Blondin et al. (2003). Second, when the shock instability can finally be identified, the matter is already convecting nonlinearly due to neutrino heating. Hence, a linear growth analysis may be inaccurate, or, at the very least, the seed perturbations for the shock-instability are the turbules and plumes of neutrino-driven convection. Third, the nonlinear phase of the shock instability brings with it secondary shock waves and the shock oscillation becomes saturated and non-periodic. By itself, the shock instability is not leading to explosion and the average radius of the outer shock ceases to increase, though the wobble and top-bottom asymmetry can still be extreme. Fourth, within the first 100-150 ms of the shock instability its behavior not only ceases to be periodic with a clear oscillation period, but is also not a simple normal mode. A new phenomenon arises. The increasing vigor of the turbulence in the interior outside of the core (< 100 km), in part generated by the fluctuations and "wagging" over the core's surface of the lower-entropy accretion streams stirring this inner region, begins to generate traveling acoustic waves, sound that propagates outward, with initial periods $\leq 5-10$ ms determined by the turbule overturn times in the interior and the timescale for the heads of the accretion plumes to traverse the latitudes of the PNS surface. Such acoustic power is a new feature in supernova theory. This is not the acoustic component of the "advective-acoustic" instability, which is a normal mode with a period near the sound travel time across the shocked region of ∼25-30 milliseconds. Rather, it is the *propagating* acoustic flux whose source begins as the turbulent energy in the roiling interior, driven by aspherical accretion of matter and entropy onto the core. This is analogous to the "forced-turbulence" source for the acoustic flux studied by Goldreich & Kumar (1988,1990) in the context of solar convection. These authors showed that the efficiency of sound generation in a driven turbulent region increases roughly as the Mach number (M) cubed [9]. The Mach numbers seen in our simulation are on average steadily rising, evolving in the inner ∼100 km from ∼0.1 to as high as ∼0.9. This turbulence is initially fed by the grossly aspherical accretion flows associated with the shock instability and the dancing accretion streams regulated by it.

However, when the acoustic flux becomes appreciable, it significantly modifies the shock instability. In our calculation, over a period from ∼350 to ∼450 ms, the motions of the shock and accretion flow transition from being dominated by the shock instability to being dominated by the core's acoustic flux. The propagating sound waves issuing from the core modify the outer flow to such an extent that the shock motion is no longer even quasi-periodic and the momentum and energy flux of the sound start to determine the flow pattern. In particular, the acoustic flux is refracted and reflected by the accretion streams and emerges very anisotropically, and more on

[9] Furthermore, they showed that the peak in the acoustic frequency spectrum is near H/v, which is close to what we witness at this stage in our simulation, where H is the characteristic turbule size and v is the characteristic turbulent speed. However, another characteristic driving timescale is the period over which the accretion streams "dance"/"flap" over the surface of the PNS. This timescale is a bit longer than H/v until the core g-mode oscillation

one side of the core than another. At the same time, the accretion streams are pushed by the momentum of the acoustic flux more and more onto the other side of the core, whichever that happens to be. The positions of the accretion streams and the average direction of the acoustic flux become anti-correlated. Figure 3 clearly shows the low-entropy accretion streams and their positioning, as well as the discontinuities in the velocity vector field that mark the emerging sound pulses. In fact, in propagating outward down the density gradient, the sound pulses steepen into shock waves, subsequent pulses catching up with and reinforcing previous pulses. From ∼400 ms after bounce, sound waves make themselves felt more and more and the resultant nested shock waves become a feature of the early supernova phenomenon.

By 500 ms after bounce, the acoustic power from the core is quite pronounced and is starting to power outflow and the beginnings of an explosion. Figure 4 depicts the temporal evolution after 100 ms of the entropy profile along the poles. The position of the outer shock, the early decay of its radius, the wobble due to the shock instability after ∼250 ms, the fact that the outer shock radii at 0° and 180° (the top and the bottom) are roughly out of phase until ∼500 ms, the entropization due to successive pulses at late times, and the onset of explosion are all clearly seen. Figure 5 depicts the evolution of the Mach number profile, also along the axis of symmetry and as a function of time. This figure recapitulates Fig. 4, showing the shock oscillations and the onset of explosion, while also showing the growth of the Mach number with time and the secondary shocks at later times. Note that despite clear evidence on this figure for a periodicity in the Mach number of the accreted matter and, hence, in the flow from ∼100 ms to ∼250 ms after bounce, the average shock radius does not increase due to a shock instability until afterwards. By ∼500 ms, one lobe of the outer shock is near 1000 km and by ∼660 ms it has reached ∼2300 km. The accretion streams are now perennially on one side of the core and the acoustic flux, while mostly emanating from the other side is radiating in all directions, except up the accretion streams themselves. Figure 3 depicts this clearly, though at ∼600 ms some matter is still infalling, particularly the lower-entropy streams. The entropy of some of the shocked matter can now be hundreds of units, due mostly to progressive shock heating by the steepening sound pulses, not the neutrinos. Starting around ∼550 ms, as the explosion commences, entropization due to these multiple shocks is clearly seen in Fig. 4.

After ∼500 milliseconds, and certainly by 550 ms, the sonic power, though its early source was the turbulence around the core region, is driven mostly by a core oscillation that is being excited by the violent accretion streams. This oscillation can be seen as early as ∼350 ms after bounce and has a period near ∼3 milliseconds, very much smaller than the sound-travel-time in the shocked cavity. It is predominantly an $\ell = 1$ g-mode of the inner ∼40 kilometers that has grown strong over a period of ∼100 ms to reach nonlinear amplitudes by ∼500 ms. This mode would have been suppressed had we excised the inner core, not performed the calculations over the full 180°, or performed the simulations in 1D interior to some convenient radius and is discussed in §5. The core oscillation is acting like a transducer for the conversion of the gravitational energy of infall into radiating acoustic power and at the later stages is a far more important source of acoustic power than the inner turbulence. Moreover, from ∼400 ms to ∼660 ms the efficiency for the conversion of accretion power into sound power is increasing. As long as the accretion continues during this phase, the core oscillation seems to be driven and the sound is emitted. After the explosion has progressed sufficiently and accretion subsides, the core oscillation decays and the sound source abates. It seems that as long as the acoustic power due to core oscillation is needed to drive the explosion, it is available. If the neutrino mechanism does not abort this scenario by inaugurating an earlier explosion, this may be a natural self-regulating mechanism for the supernova phenomenon.

4. ACOUSTIC WAVES AS THE CRITICAL POWER AND MOMENTUM SOURCE

Hydrodynamic, neutrino, convective, viscous (Thompson, Quataert, & Burrows 2005), and magnetic (Akiyama et al. 2003) mechanisms for driving core-collapse supernova explosions have all been proposed and investigated. Acoustic power is (or would be) a new paradigm. If the neutrino mechanism obtains, it needs to inaugurate explosion early, perhaps in the first 200-400 milliseconds after bounce. This is because the driving neutrino luminosity, the absorbing mantle mass, and the optical depth of this mass to the emerging neutrinos, are decreasing. The result is that the neutrino energy deposited in the gain region is inexorably diminishing. In the simulations we present here, we do not see a neutrino-driven explosion. For all the most detailed simulations by the Garching group (cf. Buras et al. 2005), except for their model s15Gio_32.a, which they exploded artificially (see also, Janka, Buras, & Rampp 2003), this is also the case. This does not mean that the neutrino mechanism does not obtain. Indeed, 1) the LANL group (cf. Fryer & Warren 2002,2004) does get neutrino-driven explosions using its gray SPH code, 2) many calculations to date may have critical flaws, and 3) accretion-induced collapse may well explode by the neutrino mechanism rather easily.

However, there are certain virtues to acoustic driving that bear mentioning. First is that while the acoustic luminosity is much smaller than the neutrino luminosity, almost all of the sound is absorbed in the mantle matter. At late times in our simulation, less than a percent of the ν_e and $\bar{\nu}_e$ neutrino luminosity is absorbed. This amounts to an neutrino absorption power of $\leq 10^{50}$ erg s^{-1}, compared with an estimated core acoustic power at the end of our calculation near $\sim 10^{51}$ erg s^{-1}. Figure 6 compares the ν_e and $\bar{\nu}_e$ neutrino luminosities, the integrated neutrino heating rate (power) in the gain region, the gravitational accretion power ($\dot{E}_{acc} \sim \frac{GM}{R}\dot{M}$), and an estimate of the acoustic power due to core g-mode oscillations. Due in part to the very complicated flow

patterns and sonic refraction and reflection, it is difficult to determine precisely this total acoustic power. However, with a simulation-motivated estimate of ∼120 ms for the acoustic damping e-folding time (τ_E) of the $\ell = 1$ core g-mode [11] and our calculated energy (E_g) in this normal mode as a function of time, we can estimate this late-time acoustic power ($\sim E_g/\tau_E$) and have included this estimate in Fig. 6. There is a time, in our calculation near ∼350−400 ms, when the absorbed neutrino power goes below the rising acoustic power.

Second, sound carries not only energy, but momentum, and this factor seems to be important in our simulations. The momentum flux for sound with the same energy flux as neutrino radiation is larger by the ratio of the speed of light to the speed of sound, which in the inner mantle regions is as much as a factor of ten. Third, acoustic power propagates from where it is generated to where it is needed; it fulfills the central requirement of a core-collapse supernova mechanism that it involve energy transfer from the bound interior PNS to the outer exploding mantle. If the acoustic power is large enough, it is the ideal transfer agent. Fourth, the acoustic source seems to grow just when the neutrino luminosity is ebbing and, importantly, it continues until explosion ensues. Fifth, the successive merger of trains of sound waves that steepen into shocks provides a non-neutrino way to entropize some of the matter and naturally achieve r-process conditions.

5. THE EXCITATION AND DAMPING OF CORE OSCILLATIONS

Within ∼200-300 ms of bounce, the inner core has reached a total baryon mass above ∼1.3 $M_\odot$. Exterior to a radius of ∼40 km, the density profile is falling off precipitously. The entropy in this inner core is of order unity (in units of Boltzmann's constant per baryon), and the outer Y_e profile has a steep negative gradient. The neutrinospheres reside in this low Y_e regime at radii of ∼30−40 km. Surrounding this inner core is a high-entropy accreting, turbulent mantle, whose entropy and Mach numbers are increasing with time. At ∼200 ms, the total accretion rate is ∼0.1 $M_\odot$ s^{-1} and is decreasing, but the temporal and spatial variations in the accretion fluxes and the ram pressures of the infalling plumes that eventually settle onto the inner core are quite large. Figure 7 shows the time evolution of the spherical harmonic weighting coefficients, a_ℓ, of a decomposition into $Y_{\ell m}$s of the fractional fluctuations of the pressure field at a radius of 35 km for $\ell = 0, 1, 2$, and 3[12]. We see in Fig. 7 the emergence of a pronounced $\ell = 1$ component, whose modulation up to ∼600 ms is at the period of the outer shock instability (∼25−30 ms).

This situation is perfect for the excitation of the normal modes of oscillation of the inner core that are analogous to classical stellar pulsations (Goldreich & Kelley 1977). Stars can execute p-modes, g-modes, and/or f-modes. The dominant restoring force for p-modes is pressure and that for g-modes is gravity. The f-modes generally have no radial nodes and are fundamentally of mixed type, though all realistic pulsational modes have some mixed character. Importantly, all the prominent modes excited in our simulations are significant admixtures of both g-type and p-type character. We have performed an analytic modal analysis of the PNS core for its structure at ∼500 ms after bounce and display the derived periods in Fig. 8. The p-mode (green dots) and g-mode (red stars) branches for each spherical harmonic angular eigenfunction ($Y_{\ell m}$) are shown here as a function of ℓ[13]. Given an ℓ, for predominantly g-modes the period increases with number of radial nodes and for predominantly p-modes the period decreases with number of radial nodes, the latter as expected for sound waves in a cavity. Generally, the shorter period (higher frequency) oscillation modes are predominantly p-modes and those at longer periods (lower frequency) are predominantly g-modes and for all modal types the period is a decreasing function of ℓ. The radial eigenfunctions of p-modes peak on the outside, while those of g-modes peak on the inside. At the boundary between the p-modes and the g-modes on Fig. 8, the modes are quite mixed, so that some of those modes might be assigned differently by others, for instance as f-modes.

The periods for most of the modes depicted in Fig. 8 are shorter than the characteristic times of pressure fluctuations and turbule overturn in the turbulent outer regions. Moreover, the dynamical times in the core-bounding region from 50 to 100 kilometers are longer than those in the core itself. In addition, though excitation by a neutrino κ-mechanism has yet to be investigated, one can show that the high-frequency p-modes would damp so quickly by sound emission that they can not be excited to significant amplitude. However, as Goldreich & Kumar (1990) have shown, the efficiency for turbulence to excite g-modes is linear in Mach number, M. As M grows, the fraction of the turbulent power around the core that is pumped into g-modes increases. Furthermore, the g-modes have the longest periods among the modes that could possibly be excited, and are, hence, the most likely to be resonantly excited by convective turbules and the waving accretion streams.

Therefore, we would expect a whole spectrum of core modes to be excited, with the g-modes eventually dominating. A variety of ℓs above 0 should be represented, but the fact that the accretion is channeled into a small number of plumes/streams (generally, in our 2D calculations, one per hemisphere at late times) means that lower values of ℓ should prevail. This is what we see in our 2D simulations. After ∼450 ms, over a period of ∼100 ms, the $\ell = 1$ dipole mode with predominantly g-type character at a period near ∼3 milliseconds emerges to significant amplitude, reaching Lagrangian displacements of ∼3 km. This core mode has a radial node near 6−10 km, though it has a few nodes of p-type character further out. This mode corresponds to the analytic mode circled in Fig. 8[14]. It damps by the emission of acoustic power, sound waves, with an oscillator Q value ($= \omega\tau_E$, where τ_E is the e-folding time for energy loss) near ∼200.

[11] One can use the FWHM of the power spectrum of the core pressure fluctuations around the 3−ms mode or the early growth rate of the core oscillation kinetic energy to get a handle on this

[13] Without rotation, we expect the modes to be degenerate in m.

[14] There are no $\ell = 0$ g-modes, and no g-modes without nodes, since this would not conserve momentum. Note that the $\ell = 1$ p-mode without a radial node would be a zero-frequency core trans-

In its nonlinear phase after ∼580 ms, the total pulsation energy is $\sim 10^{50}$ ergs and the radiated acoustic power is near $\sim 10^{51}$ erg s^{-1}. Figure 9 depicts the time evolution of the spectrum of pressure fluctuations at a radius of 30 km. On this frequency-time plot one sees the emergence of the 3−ms core g-mode oscillation to dominate after ∼450 ms, as well as a number of other periodicities (modes) of lesser strength. For instance, the mode seen in Fig. 9 near ∼675 Hz is an $\ell = 2$ harmonic.

Though the radiation pattern we actually observe is quite anisotropic and variable, and the sound is severely refracted and diverted by the complicated accretion/turbulent flow patterns, to gain insight one can estimate the dipole acoustic power ($\dot{E}_s^{\ell=1}$) radiated by a sphere of radius R executing periodic linear translational motion (wobbling) of amplitude ΔR with period P in a gas of density ρ and sound speed c_s. This is given by (Landau & Lifshitz 1959):

$$\dot{E}_s^{\ell=1} = \frac{2\pi}{3}\rho c_s R^2 u_0^2 \frac{(\kappa R)^4}{(4+(\kappa R)^4)} \qquad (1)$$

$$\sim 4\times 10^{51}\mathrm{erg\,s^{-1}}\rho_{12}\Big(\frac{c_s}{3\times 10^9\mathrm{cm\,s^{-1}}}\Big)\Big(\frac{R}{30\,\mathrm{km}}\Big)^2\Big(\frac{\Delta R}{3\,\mathrm{km}}\Big)^2\Big(\frac{3\,\mathrm{ms}}{P}\Big)^2,$$

where $\rho_{12} = \rho/10^{12}\,\mathrm{g\,cm^{-3}}$, κ $(= \omega/c_s)$ is the wave number of the sound generated, ω is the angular frequency of the oscillation $(= 2\pi/P)$, and $u_0 = \omega\Delta R$. The numbers given in eq. (1) are representative quantities for the problem at hand and the impedance term $((\kappa R)^4/(4+(\kappa R)^4))$ has been set to 1/5. Since in reality there are complicated density and sound speed profiles, the application of eq. (1) is no more than a very crude approximation. Nevertheless, we see from simple analytics that even for small values of ΔR the acoustic power radiated by core oscillations can be quite large, and can be of importance in the supernova context. At high oscillation frequencies and surrounding pressures, even small amplitude oscillations generate competitive acoustic radiation. This is what we see in the more detailed simulations, in which we derive acoustic powers due to core oscillations of $\sim 10^{51}$ erg s^{-1}. Almost all of this power is absorbed in the mantle and is potentially available to the explosion. This is to be compared (see Fig. 6) with the accretion power at late times of:

$$\dot{E}_{acc} = \frac{GM}{R}\dot{M} \sim 10^{52}\,\mathrm{erg\,s^{-1}}\Big(\frac{M}{1.4M_\odot}\Big)\Big(\frac{\dot{M}}{0.1M_\odot\mathrm{s^{-1}}}\Big)\Big(\frac{30\,\mathrm{km}}{R}\Big). \qquad (2)$$

Core oscillations can therefore convert accretion power into acoustic power with some efficiency. In our baseline simulation at the same epoch, L_ν(total) is $\sim 5\times 10^{52}$ erg s^{-1} and $L_{\nu_e/\bar{\nu_e}}$ is $\sim 2\times 10^{52}$ erg s^{-1}. In contrast, $L_{\nu_e/\bar{\nu_e}}\times\tau_\nu$ (where τ_ν is the gain-region optical depth to $\nu_e/\bar{\nu}_e$ neutrino absorption) is $<10^{50}$ erg s^{-1}. These power/luminosity comparisons, also depicted in Fig. 6, highlight the problem, and its potential solution.

Importantly, what we see in our simulations is the *self-excitation* of the core g-mode; the inner core plus inner accretion region is a self-excited oscillator. The interaction between the sound pressure and the accretion streams (see, e.g., Fig. 3) that results in an anticorrelation at late times between the angular positions of the accretion streams and the average direction of the emit-

clear features of our simulations. However, the flow fields are quite complicated and variable. What we have yet to determine is whether the sound modulates the exciting accretion streams to create a feedback loop with gain and a time delay, the classic context for a feedback amplifier, quartz crystal oscillator, acoustic feedback oscillator, klystron, or edgetone oscillation. This possibility requires further exploration, but is intriguing.

The core oscillations are acting like a transducer for the conversion of the gravitational energy of accretion into acoustic power. The oscillation continues as long as the accretion continues, ensuring that acoustic power persists until accretion stops. This may be one means by which a supernova, and its energy, are self-regulating, given a progenitor structure. The halt of accretion is one manifestation of explosion. In fact, the accretion streams, sequestered predominantly on one side of the inner core, pump up the core oscillation and store energy in it like a battery or capacitor. Even after accretion subsides the energy in the core motion will continue to be damped by acoustic radiation, neutrino viscosity, and gravitational radiation, the former being dominant. However, as the gas pressure around the core decreases due to explosion, because of the increasing impedance mismatch between the core and the expanding mantle, the acoustic damping time is bound to increase. We have yet to calculate this effect, but the core may oscillate for a "long time." However long it takes, most of the oscillation energy will eventually be "discharged" sonically into the supernova explosion.

The angular distribution of the emitted sound is fundamentally aspherical. The actual modal periods depend upon the nuclear EOS used, and will be different when general relativity is incorporated into the calculations. Relativity will decrease the period and increase the pressures that surround the core, but it will also decrease the core size. Therefore, how relativity will alter the acoustic power is not yet clear. Furthermore, how the accretion streams will behave in 3D, where the pattern of infalling plumes and its evolution are as yet unknown, remains one of the major uncertainties of our acoustic model. A rotation axis may set a direction and render important aspects of a 3D simulation like those in a 2D simulation. This is what is suggested in the linear analysis of Miralles et al. (2004) and what one would conjecture from the generic alignment effects on convective plumes of the Sølberg-Hoiland instability. Otherwise, there may be a spectrum of modes that are not degenerate in azimuth and in "magnetic quantum number" m. In addition, though we did not see much power in $\ell = 2$ modes, they may contribute more in the real 3D situation. Nevertheless, from our calculations, uniquely allowing as they do core motion on a 2D grid, the excitation of non-radial core g-modes seems to be a natural consequence of the later stages of stellar collapse.

6. THE ROLE OF NEUTRINOS

In the baseline simulation we have performed for this paper, despite the fact that it involves an 11-$M_\odot$ progenitor with a steep outer density profile and despite the appearance and strengthening of neutrino-driven convection in the first ∼200 ms after bounce, we do not witness a neutrino-driven explosion. This does not mean that

may be that different input physics, different progenitors, an improved numerical technique, or not employing the MGFLD approximation could result in a neutrino-driven explosion. Since they should accrete their outer boundaries quickly within less than ∼100 ms after bounce, ONeMg white dwarfs that achieve the Chandrasekhar mass and collapse due to accretion from a companion (accretion-induced collapse, AIC) can't avoid exploding in the early post-bounce stages before the shock instability and core acoustic sources turn on. Nevertheless, with our fully 2D multi-group code, general Poisson solver, and adequate energy-group and spatial resolution, shock stagnation is prolonged until long after the first peak in the average shock radius (near 150-200 km) and its subsequent initial decay. In the past, this peaking and decay were taken as signatures of a fizzle.

However, if our result is an adequate representation of Nature, then what is the role of neutrinos in the more-delayed sound-driven mechanism we have discovered? First, neutrinos still deposit energy in a gain region. Figure 6 depicts not only the neutrino luminosities, but the neutrino power deposited in the gain region as a function of time. Hence, neutrinos will certainly contribute a fraction of the explosion energy. Second, from the work of Foglizzo and collaborators and of Blondin, Mezzacappa, & DeMarino (2003), we expect that the shock instability requires a large shock height and a large ratio between the speeds of sound at the core and at the shock. Neutrino-driven convection results in larger shock radii after the stalling of the shock than obtain without neutrino-driven convection. Nevertheless, the shock instability can't commence until the inner core slows its quasi-static contraction, a phenomenon slaved to neutrino and lepton losses. Third, neutrino heating of the accreted and shocked material that goes through the gain region is one reason the entropies around the core increase after ∼200 ms after bounce. The other reason is enhanced, multiple shock heating due to the shock instability. Higher entropies and larger entropy perturbations result in larger overpressures during the earlier turbulence-driven acoustic flux phase seen in our simulations before the core oscillation becomes vigorous. Fourth, neutrinos are responsible for the failure of the direct mechanism for progenitors less massive than ∼20 $M_\odot$[15]. If this mechanism succeeded, then the gravitational mass of the residual neutron star very likely would be too small to explain observed pulsar masses. Fifth, the absorption of ν_e and $\bar{\nu}_e$ neutrinos by the ejecta may be responsible for ensuring that its Y_e is not too small to be consistent with nucleosynthesic constraints (Frohlich et al. 2005; Pruet et al. 2005). Furthermore, Y_es above 0.5 that are possible only due to an excess of ν_e absorption over $\bar{\nu}_e$ absorption might be needed to explain the rp-process isotopes. However, we find that the mass of the core ejecta in our acoustic-power-driven explosion is less than 0.01 $M_\odot$ and that there may not be as much of a problem with anomalously neutron-rich ejecta for the lowest-mass massive stars. Finally, neutrino cooling of the multiple shocks emanating from the core slightly diminishes the acoustic energy that in our scenario ultimately powers the supernova. Determining the correct magnitude of this negative effect will be important and might require better neutrino transfer and better weak-interaction physics than we have incorporated into our 2D MGFLD approach.

In the calculations we present in this paper, neutrino transport and weak-interaction physics are crucially important, but are not the critical factors in the explosion mechanism. Anisotropic neutrino radiation pressure may in some circumstances 1) affect the core oscillations, and 2) contribute an integrated net impulse to the PNS and, therefore, a kick. However, in our baseline model, with the single progenitor on which we focus, such effects are subdominant and the direct role of neutrinos is subordinate to the other factors described in §3 and §5.

7. DISCUSSION AND CONCLUSIONS

In this paper, we present a new mechanism for core-collapse supernova explosions that focusses on the acoustic power generated in the core region. The strength, radiation pattern, and character of the emergent sound are influenced by the shock instability that arises after ∼200 ms, but this instability is not the agent of explosion. Rather, it is the acoustic power generated first in the turbulent region around the inner PNS core and then through the excitation and sonic damping of core g-mode oscillations. An $\ell = 1$ mode grows at late times to be prominent around ∼500 ms after bounce, though it is in evidence as early as ∼300 ms after bounce. In our Newtonian simulation, its period is ∼3 ms. At the end of the calculation, this core g-mode contains $\sim 10^{50}$ ergs, is radiating sound into the exploding mantle at a rate near $\sim 10^{51}$ erg s^{-1}, and has a Q-value of ∼200. At late times, but before explosion, the accreting protoneutron star is a self-excited oscillator, "tuned" to the most easily excited core g-mode. After the acoustic power becomes strong, the average direction of the radiated sound and the angular positions of the exciting plumes outside the core are anti-correlated. The possibility that the PNS-core/accretion-stream system is a feedback amplifier is an intriguing notion suggested by our simulations, but that has yet to be properly explored. Since core $\ell = 0$ modes are not excited to an appreciable degree, the driving acoustic radiation pattern is fundamentally anisotropic and the initial phase of the explosion is *unipolar*. In addition, due to the extreme breaking of spherical symmetry, this model manifests simultaneous accretion and explosion. The ultimate source of the acoustic power is the gravitational energy of infall and the core oscillation acts like a transducer to convert this accretion energy into sound.

An advantage of the acoustic mechanism is that acoustic power does not abate until accretion subsides, so that it is available as long as it is needed. This is not the case for neutrinos, whose luminosities and mantle heating rates inexorably decrease at late times. Hence, this may be the long-sought-after self-regulating mechanism of the supernova energy and, being a function of the accretion rate, is determined mainly by the progenitor density structure, with some ambiguity due to the sensitivity to initial conditions in chaotic flows and due to rotation. Furthermore, unlike neutrinos, sound pulses that steepen into shock waves are almost completely absorbed in the baryonic outer mantle. Moreover, sound deposits net

[15] For progenitors more massive, nuclear photodissociation alone

tion rates that were thought to inhibit explosion in the neutrino-driven mechanism are not a disadvantage in the acoustic model. In fact, the very accretion that might be inhibiting the neutrino mechanism facilitates the acoustic mechanism, but at later times. Furthermore, by their nature the accretion funnels constitute a disproportionate share of the infalling material. The result is that while at the same time these streams are exciting the core oscillations accretion from the other directions is weaker, thereby presenting less of an obstacle in those directions to eventual explosion. In our calculation with the 11-$M_\odot$ progenitor, the delay to explosion is $\sim$550 ms. This is longer than the delay traditionally associated with the onset of multi-D neutrino-driven explosions ($\sim$200$-$300 ms).

The baryon mass of our remnant neutron star is $\sim$1.42 $M_\odot$, with a gravitational mass near $\sim$1.3 $M_\odot$. This is close to what is canonically expected from measured values. Had the core exploded much earlier, the mass remaining might have been uncomfortably lower.

The successive superposition of multiple shocks and the shock-shock interactions during the shock instability phase lead naturally to higher entropies in a fraction of the supernova ejecta. In our baseline calculation, entropies higher than 300 were achieved. High entropies may be a partial consequence of the thin accreting envelope, suggesting that higher-mass progenitors would not so easily yield such high numbers. Since the supernova energy, kick velocities, and ejecta entropies are all dependent in our acoustic model on the accretion regime, these quantities may in fact be correlated along the progenitor mass continuum, with lower-mass progenitors having low explosion energies, some r-process nucleosynthesis, and weak kicks, and higher-mass progenitors having higher explosion energies, no r-process, and significant kicks. Observations do suggest that lower mass massive stars are the likely sites of the r-process (Mathews, Bazan, & Cowan 1992) and that supernova energies might span a wide range (Hamuy 2003). Be that as it may, the progenitor dependence of the supernova explosion systematics is an important aspect of the supernova story and one that we have yet to explore in the context of this new mechanism.

Though we find that an $\ell = 1$ g-mode eventually dominates, $\ell = 2$ and $\ell = 3$ modes and harmonics are in evidence and there is also likely to be nonlinear mode-mode coupling. Unlike $\ell = 1$ modes, $\ell = 2$ modes will generate gravitational radiation and will do so at characteristic frequencies (!) that is a function of the EOS, relativity, and the PNS structure. Using the results from earlier quasi-static PNS cooling calculations, Ferrari et al. (2003) calculated its g-mode frequencies and their evolution. Including as they do general relativity, Ferrari et al. derive frequencies for the fundamental g-modes that are slightly higher than we derive using our Newtonian code, and find that these frequencies, after an initial rise, evolve to lower values. Our calculations recapitulate exactly this initial rise (Fig. 9) and subsequent decay after $\sim$670 ms (not shown in Fig. 9). The total energy radiated in gravitational waves from this non-rotating 11-$M_\odot$ model is $\sim 10^{-8}$ $M_\odot$ equivalent (Ott et al. 2005, in preparation). Hence, in the excitation of normal modes in the supernova context, we may have a direct signature

Our calculations are Newtonian and were performed in 2D. Relativity and a different nuclear EOS (Ferrari et al. 2003) will change the frequencies of the core modes and the efficiency of sound generation, the latter in ways that are not yet obvious. Three-dimensional simulations are likely to be different from 2D simulations, manifesting more realistic plume structures. The 2D/3D difference is the major unknown and uncertainty in our scenario. However, it would be difficult to suppress in 3D the excitation of core g-modes and the generation of acoustic radiation that in 2D becomes so pronounced. Furthermore, even slight rotation may set a natural axis for the evolution in 3D. Otherwise, more subtle initial conditions will break the symmetry.

We have also performed a simulation that restricts the hydrodynamics to a 90-degree wedge, with a reflecting boundary at the equator, as opposed to operating in the full 180-degree domain. In this case, we see that the $\ell = 1$, 25-30 ms wobble due to the shock instability is completely suppressed. However, instead of arising near 200-250 ms after bounce, the shock instability starts later, around 450-500 ms after bounce, and in an $\ell = 2$ mode. Before that, the shock maintains a roughly spherical shape. Though the delay is much longer, the shock executes small-amplitude, long-period $\ell = 2$ motions until roughly $\sim$650 ms after bounce, at which time the shock instability becomes vigorous. Just before that, near $\sim$600 ms, the PNS starts to radiate sound waves from a predominantly $\ell = 2$ core g-mode with a $\sim$400 Hz frequency (see Fig. 8). Clearly, 90-degree calculations suppress an important component of the supernova story, but just as clearly, the same instability and oscillation phenomena, though dominated by $\ell = 2$ morphology, eventually arise. It just takes longer for $\ell = 2$ modes to grow.

It is important to list the reasons the acoustic phenomena we have identified and presented in this paper were not seen before. First, most calculations were stopped after the shock radius first subsided around 200-300 ms after bounce, but before the shock instability was much in evidence, and before turbulence around the core could generate significant acoustic power. Second, those calculations that were not stopped early were continued because they experienced an early neutrino-driven, multi-D explosion. Such an explosion arose either naturally from the particular code being used, or was artificially produced. If the explosion commences early, the PNS core oscillations are not excited to useful amplitudes and the shock instability is more mild. Third, and most importantly, to date all other grid-based supernova codes have conducted calculations either with the cores excised, handled in 1D, or on a $\sim 90^\circ$ wedge, thereby completely suppressing core oscillations and the resulting $\ell = 1$ acoustic flux. Such procedures can even muffle the acoustic flux generated in the turbulent inner "convective" zones. As a result of some combination of the reasons above, no previous supernova simulations, before those using VULCAN/2D, could have discovered the acoustic driving and core oscillation mechanism.

Therefore, one key to the discovery of this potentially important mechanism was the computational liberation of the inner core to execute its natural multi-dimensional motions. Another key was patience to per-

better neutrino and weak-interaction physics, full 3D radiation/hydrodynamic simulations, multi-group/multi-*angle* simulations, a new suite of progenitor models, the use of other massive-star progenitors (we have here studied only one), or some qualitatively important flaw in our approach or implementation will alter our conclusions here. The role of rotation must be explored, for both the neutrino and the acoustic models. Interestingly, when magnetic fields are incorporated into the calculations, the generation of Alfvén waves at the core oscillation frequency might prove to be another power source for the supernova (S. Woosley, private communication).

The multi-D neutrino-driven mechanism may still obtain, and likely does so for AIC systems. Moreover, it may be that some supernovae explode by the neutrino mechanism[16], while others, if the neutrino mechanism fizzles, explode by the acoustic mechanism or an MHD-jet mechanism (Akiyama et al. 2003), though the latter requires very rapid rotation that may not be available in the generic core-collapse supernova context[17]. However, though unlikely to be correct in detail, our calculations and analysis may be pointing to important new phenomena in the theory of core-collapse supernovae that have hitherto been overlooked. Much remains to be done, including the determination of the progenitor-mass and -profile dependence, explorations in 3D with neutrino transport, and verification and scrutiny by other groups. Nevertheless, we believe that the new lines of investigation we have opened up in this paper, and the potential of the acoustic mechanism interpreted broadly, should stimulate many future studies in this central problem in theoretical astrophysics.

We thank Rolf Walder, Thierry Foglizzo, Todd Thompson, Itamar Lichtenstadt, Stan Woosley, Casey Meakin, Chris Fryer, and John Blondin for fruitful discussions and their insight. We acknowledge support for this work from the Scientific Discovery through Advanced Computing (SciDAC) program of the DOE, grant number DE-FC02-01ER41184, and from the NSF under grant AST-0504947. E.L. thanks the Israel Science Foundation for support under grant # 805/04, and C.D.O. thanks the Albert-Einstein-Institut for providing CPU time on their Peyote Linux cluster. This research used resources of the National Energy Research Scientific Computing Center, which is supported by the Office of Science of the U.S. Department of Energy under Contract No. DE-AC03-76SF00098. Finally, we thank Don Fisher, Youssif Al-nashif, and Moath Jarrah for their help generating both the color stills and the movies associated with this work.

[16] See the papers by Janka et al. 2005ab for the suggestion that the neutrino mechanism might still obtain for the lowest mass massive stars when the full 180° computational domain (even without liberating the core to execute oscillations) and state-of-the-art Boltzmann transport are incorporated. These authors seem to see the onset of explosion for an 11.2-$M_\odot$ model from Woosley, Heger, & Weaver (2002). Interestingly, this model has a small iron core mass of ∼1.25 $M_\odot$, a density cliff near 1600 km, and a much steeper mantle density gradient around 1000-2000 km than the 11-$M_\odot$ model from Woosley & Weaver (1995) upon which we focus in this paper.

[17] However, such rapid rotation might enable the MHD scenario for hypernovae and long-duration gamma-ray bursts.

REFERENCES

Akiyama, S., Wheeler, J.C., Meier, D.L., & Lichtenstadt, I. 2003, ApJ, 584, 954 2003ApJ...584..954A

Arnett, W.D. 1966, Can. J. Phys., 44, 2553

Bethe, H. & Wilson, J. R. 1985, ApJ, 295, 14

Blondin, J.M., Mezzacappa, A., & DeMarino, C. 2003, ApJ, 584, 971

Bruenn, S.W. 1985, ApJS, 58, 771

Bruenn, S.W. & Dineva, T. 1996, ApJ, 458, L71

Bruenn, S.W., Raley, E.A., & Mezzacappa, A. 2005, astro-ph/0404099

Buras, R., Rampp, M., Janka, H.-Th., & Kifonidis, K. 2003, Phys. Rev. Lett., 90, 241101

Buras, R., Rampp, M., Janka, H.-Th., & Kifonidis, K. 2005, astro-ph/0507135

Burrows, A., Hayes, J., & Fryxell, B.A. 1995, ApJ, 450, 830

Burrows, A., Young, T., Pinto, P., Eastman, R. & Thompson, T. 2000, ApJ, 539, 865

Burrows, A. & Thompson, T.A. 2004, "Neutrino-Matter Interaction Rates in Supernovae: The Essential Microphysics of Core Collapse," in *Core Collapse of Massive Stars*, ed. C. Fryer (Kluwer Academic Press; 2004), p. 133.

Colgate, S.A. & White, R.H. 1966, ApJ, 143, 626

Dessart, L., Burrows, A., Livne, E., & Ott, C.D. 2005, submitted to ApJ, astro-ph/0510229

Ferrari, V., Miniutti, G., & Pons, J.A. 2003, MNRAS, 342, 629

Foglizzo, T. 2001, Astron. Astrophys. , 368, 311

Foglizzo, T. 2001, Astron. Astrophys. , 392, 353

Foglizzo, T. & Tagger, M. 2000, Astron. Astrophys. , 363, 174

Foglizzo, T., Galletti, P., & Ruffert, M. 2005, Astron. Astrophys. , 435, 397

Foglizzo, T., Scheck, L., & Janka, H.-T. 2005, astro-ph/0507636

Frohlich, C., Hauser, P., Liebendörfer, M., Martinez-Pinedo, G., Thielemann, F.-K., Bravo, E., Zinner, N.T., Hix, W.R., Langanke, K., Mezzacappa, A., & Nomoto, K. 2005, astro-ph/0410208

Fryer, C.L. & Warren, M. 2002, ApJ, 574, L65

Fryer, C.L. & Warren, M. 2004, ApJ, 601, 391

Goldreich, P., & Keeley, D.A. 1977, ApJ, 212, 243

Goldreich, P., & Kumar, P. 1988, ApJ, 326, 462

Goldreich, P., & Kumar, P. 1990, ApJ, 363, 694

Hamuy, M. 2003, ApJ, 582, 905

Herant, M., Benz, W., Hix, W.R., Fryer, C.L., & Colgate, S.A. 1994, ApJ, 435, 339

Hoffman, R.D., Woosley, S.E., Fuller, G.M., & Meyer, B.S. 1996, ApJ, 460, 478

Janka, H.-T. & Müller, E. 1996, Astron. Astrophys. , 306, 167

Janka, H.-T., Buras, R., & Rampp, M. 2003, Nucl. Phys. A, 718, 269

Janka, H.-T., Buras, R., Kifonidis, K., Marek, A., & Rampp, M. 2005, in Cosmic Explosions, On the 10th Anniversary of SN1993J. Proceedings of IAU Colloquium 192, edited by J.M. Marcaide and Kurt W. Weiler, Springer Proceedings in Physics, vol. 99. (Berlin: Springer), p.253 (astro-ph/0401461)

Janka H.-Th., Buras R., Kitaura Joyanes F.S., Marek A., Rampp M., Scheck L. 2005, "Neutrino-driven supernovae: An accretion instability in a nuclear physics controlled environment," in Proceedings of the 8th International Symposium on Nuclei in the Cosmos, Vancouver, Canada, July 19–23, 2005, Nuclear Physics A, 758, 19–26

Landau, L.D. & Lifshitz, E.M. 1959, Fluid Mechanics, Pergamon Press Ltd., Oxford

Liebendörfer, M., Mezzacappa, A., Thielemann, F.-K., Messer, O. E. B., Hix, W. R., & Bruenn, S.W. 2001, Phys. Rev. D, 63, 103004

Livne, E. 1993, ApJ, 412, 634

Livne, E., Burrows, A., Walder, R., Thompson, T.A., and Lichtenstadt, I. 2004, ApJ, 609, 277
Mathews, G.J., Bazan, G., & Cowan, J.J. 1992, ApJ, 391, 719
Mayle, R. & Wilson, J. R. 1988, ApJ, 334, 909
Miralles, J.A., Pons, J.A., & Urpin, V. 2004, Astron. Astrophys. , 420, 245
Ott, C.D., Burrows, A., Livne, E., & Walder, R. 2004, ApJ, 600, 834
Pruet, J., Woosley, S.E., Buras, R., Janka, H.-T., & Hoffman, R.D. 2005, ApJ, 623, 325
Rampp, M. & Janka, H.-T. 2000, ApJ, 539, L33
Rampp, M. & Janka, H.-Th. 2002, Astron. Astrophys. , 396, 331
Scheck, L., Plewa, T., Janka, H.-Th., Kifonidis, K., & Müller, E. 2004, Phys. Rev. Lett., 92, 011103
Shen, H., Toki, H., Oyamatsu, K., & Sumiyoshi, K. 1998, in "Neutron Stars and Pulsars: Thirty Years after the Discovery," Proceedings of the International Conference on Neutron Stars and Pulsars, edited by N. Shibazaki et al., (Tokyo, Japan: Universal Academy Press, Frontiers science series, no. 24), p.157
Strack, P. & Burrows, A. 2005, Phys. Rev. D, 71, 093004, 2005
Swesty, F.D., & Myra, E.S. 2005, astro-ph/0506178
Swesty, F.D., & Myra, E.S. 2005, astro-ph/0507294
Thompson, T.A., Burrows, A., & Pinto, P.A., 2003, ApJ, 592, 434
Thompson, T.A., Quataert, E., & Burrows, A. 2005, ApJ, 620, 861
Walder, R., Burrows, A., Ott, C.D., Livne, E., Lichtenstadt, I., & Jarrah, M. 2005, ApJ, 626, 317
Wilson, J.R. 1985, in Numerical Astrophysics, ed. J. Centrella, J. M. LeBlanc, R. L. Bowers, (Boston: Jones & Bartlett), p. 422
Wilson, J.R. & Mayle, R. 1988, Phys. Rep., 163, 63
Wilson, J.R. & Mayle, R. 1993, Phys. Rep., 227, 97
Woosley, S.E. & Hoffman, R.D. 1992, ApJ, 395, 202
Woosley, S.E., Wilson, J.R., Mathews, G.J., Hoffman, R.D., & Meyer, B.S. 1994, ApJ, 433, 229
Woosley, S.E. & Weaver, T.A. 1995, ApJS, 101, 181
Woosley, S.E., Heger, A., & Weaver, T.A. 2002, Rev. Mod. Phys., 74, 1015

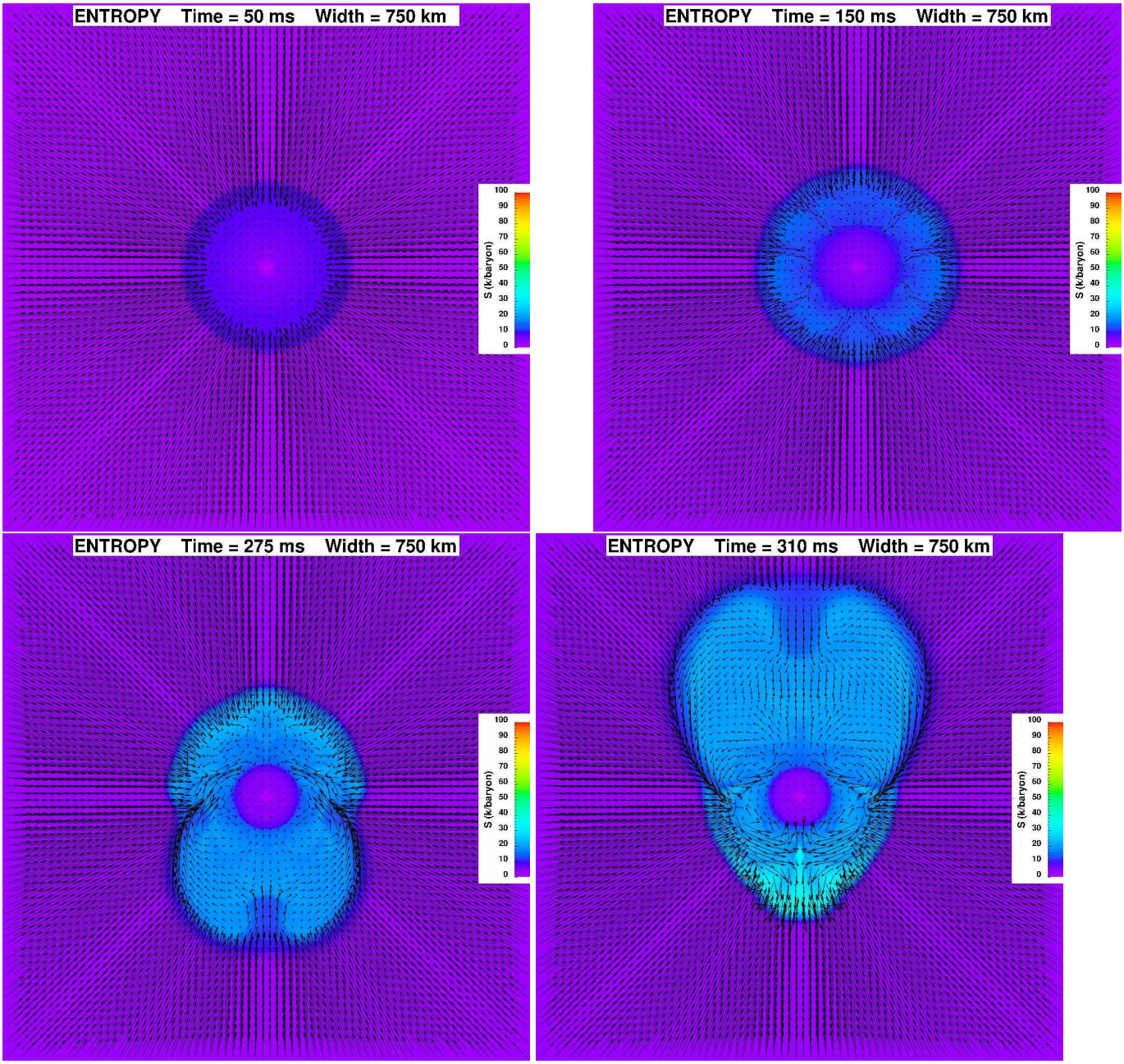

FIG. 1.— Colormap stills of the entropy, taken at 50 (top left), 150 (top right), 275 (bottom left), and 310 ms (bottom right) past core bounce, with velocity vectors overplotted. Here "Width" refers to the diameter through the middle; the radius through the middle is 375 kilometers. Note that on this figure, as well as on Fig. 2, for ease of comparison between panels the same colormap is used. It extends up to 100 units (red), above which it saturates (See text for discussion). These calculations have been done for a full 180° and the axis of symmetry is vertical.

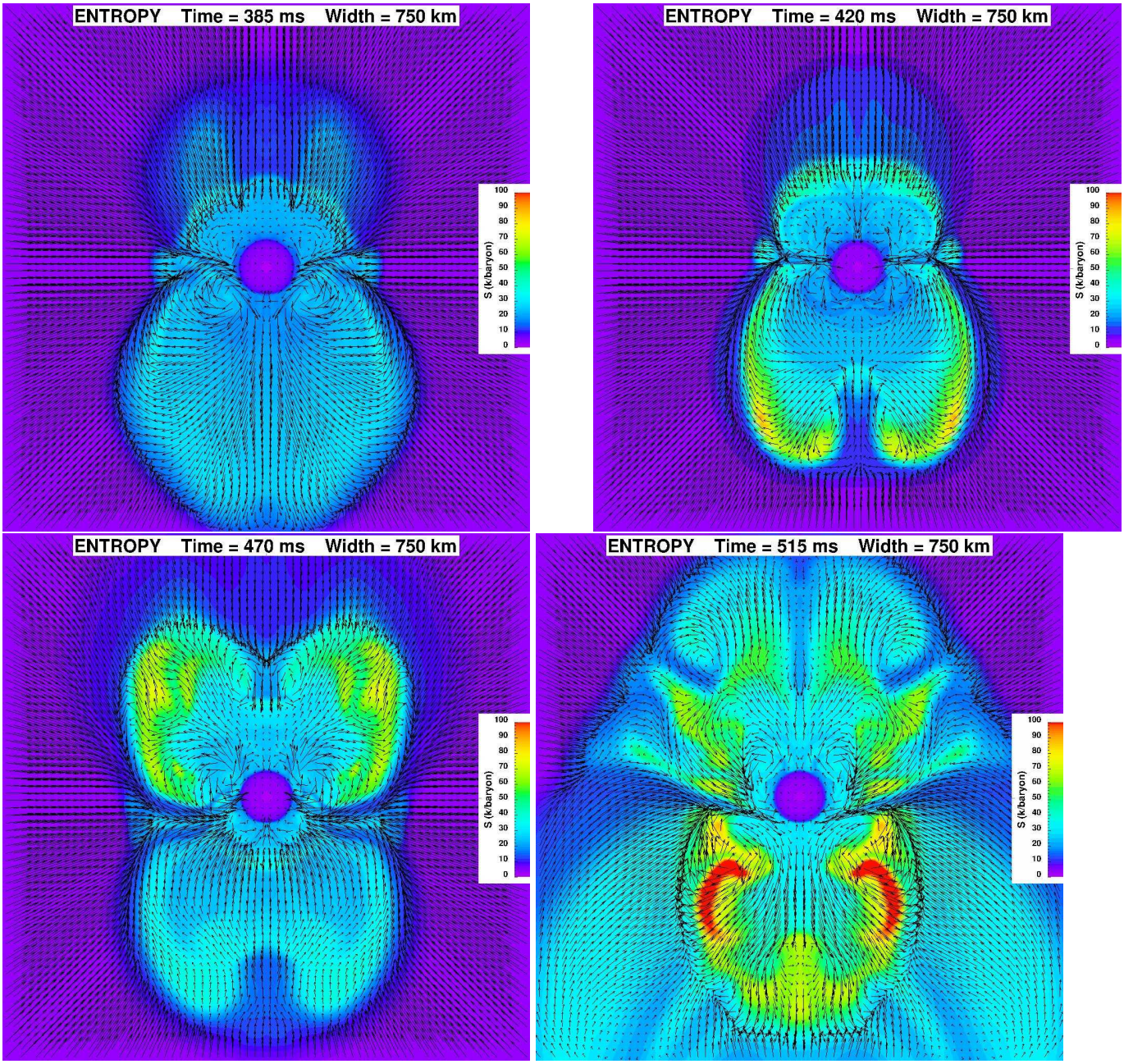

FIG. 2.— Same as Fig. 1, but this time showing the entropy at 385 (top left), 420 (top right), 470 (bottom left), and 515 ms (bottom right) past core bounce (See text for discussion).

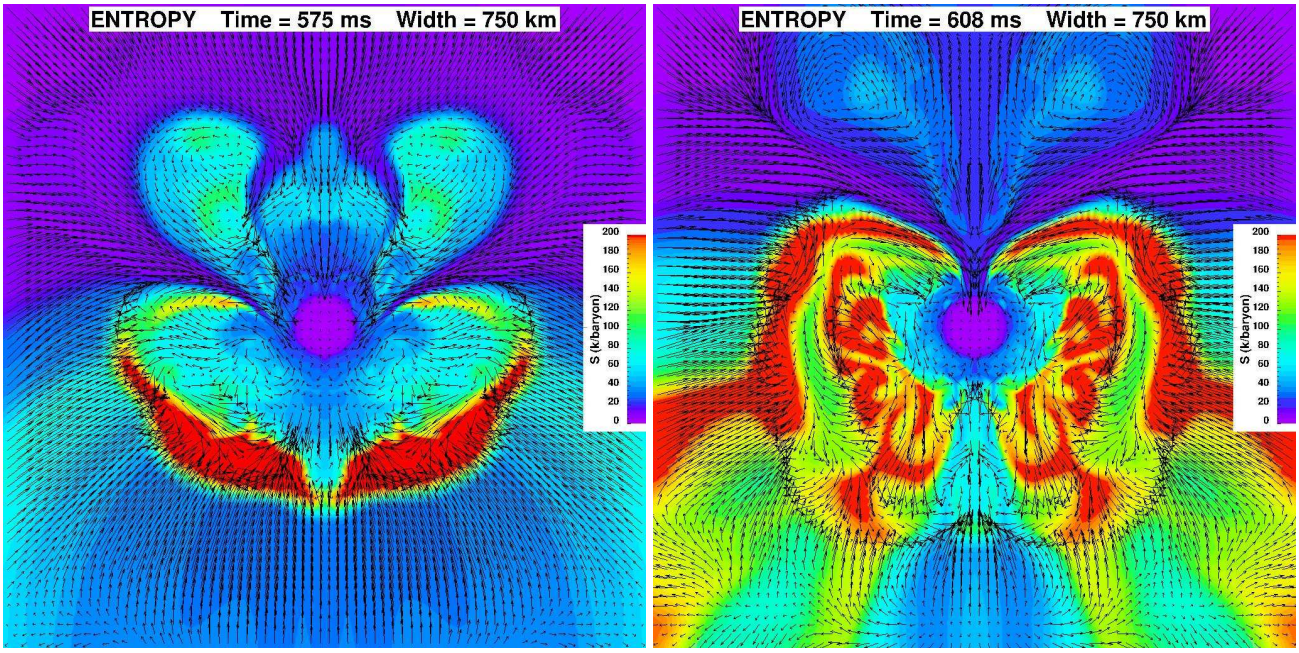

FIG. 3.— Same as Fig. 1, but this time showing the entropy at 575 (left) and 608 ms (right) past core bounce. Note the acoustic waves emanating from the core, most easily seen in the velocity vector field. The color map extends to entropies of 200 (red), and then saturates for entropies beyond 200. The low-entropy accretion streams that are exciting the core g-mode are clearly seen (see text for discussion).

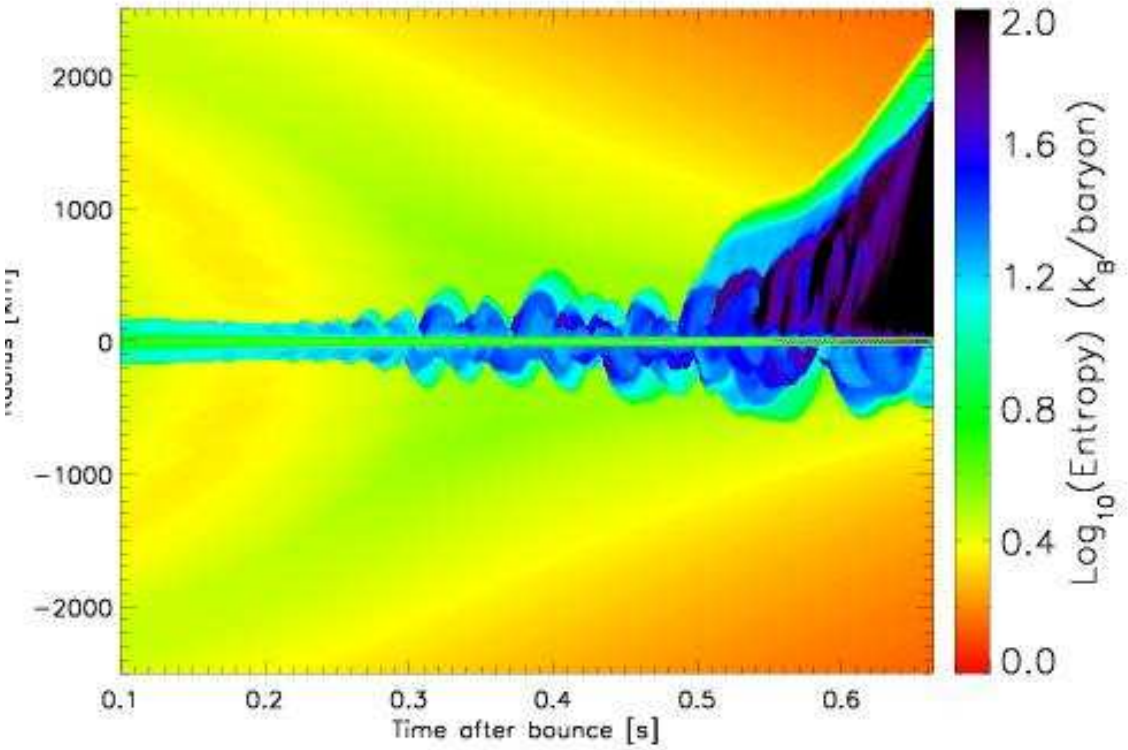

FIG. 4.— Time evolution, from 100 ms to ∼660 ms after core bounce, of the entropy (logarithmic scale) along the axis of symmetry, i.e., at $r = 0$ or latitudes $\pm 90^{o}$, and covering the inner 2500 kilometers of the grid. An entropy ceiling of 100 has been adopted.

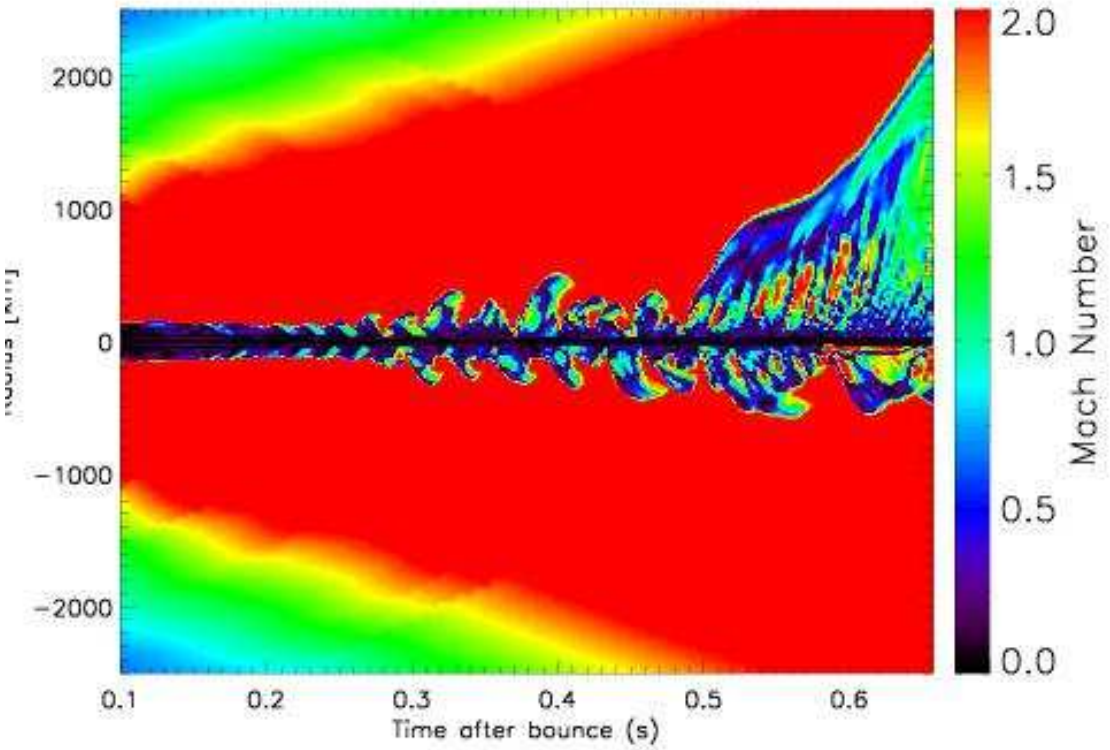

FIG. 5.— Time evolution, from 100 ms to ∼660 ms after bounce, of the Mach number along the axis of symmetry, i.e., at $r = 0$ or latitudes $\pm 90^{\circ}$, and covering the inner 2500 kilometers of the grid. Note how clearly the multiple secondary shocks emerging at late times can be discerned and that the displayed Mach number saturates at a value of two.

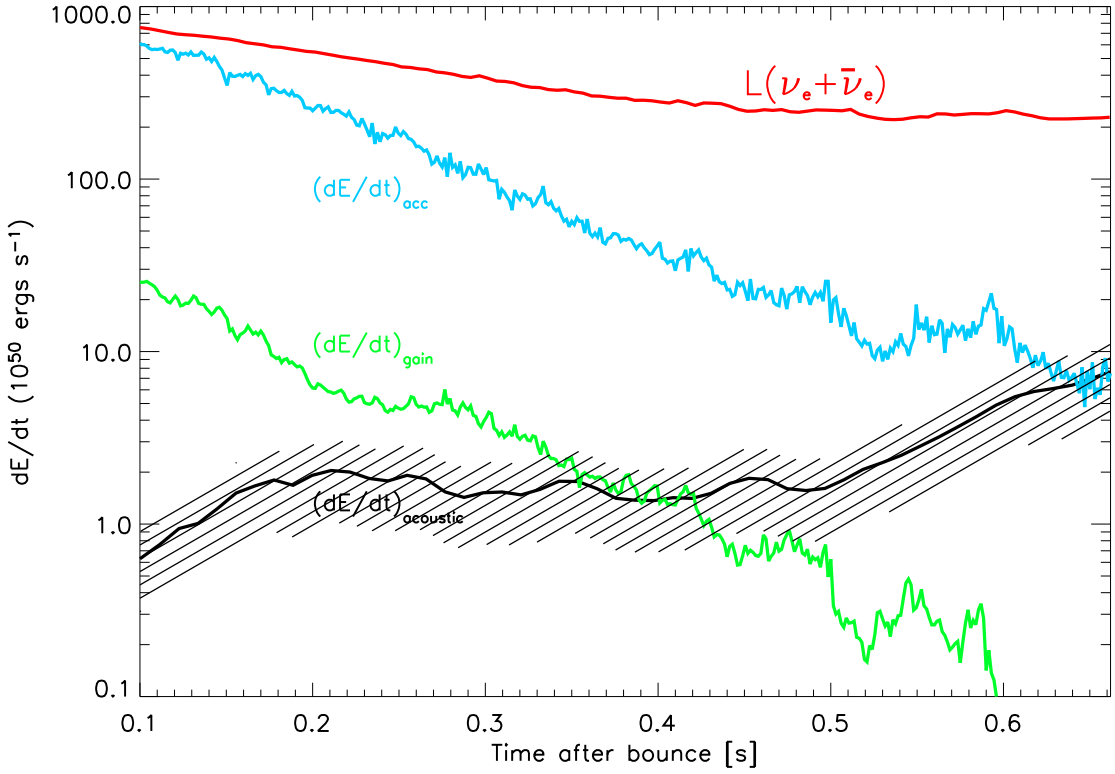

FIG. 6.— Time evolution, after core bounce, of the sum of the ν_e and $\bar{\nu}_e$ neutrino luminosities ($L(\nu_e + \bar{\nu}_e)$, red line); the gravitational energy of the accreted material (blue) through a radius R =35 km, defined as $(dE/dt)_{\rm acc} = \frac{GM_R}{R}\dot{M}_R$, where M_R is the mass interior to R and $\dot{M}_R$ the mass accretion rate through R; the net energy deposited by neutrinos in the gain region (green), defined as $(dE/dt)_{\rm gain} = \int_\Omega \varepsilon(R,\theta) dm(R,\theta)$, where Ω is the gain region, $\varepsilon(R,\theta)$ is the net neutrino heating rate, and $m(R,\theta)$ is the mass of the cell at (R,θ); and the acoustic power ($(dE/dt)_{\rm acoustic}$) radiated by the core oscillation. This is approximated here by the ratio E_g/τ_E, where E_g is the total g-mode energy interior to a radius of 40 km and τ_E is the decay time of the core pulsation, taken as 120 ms. The default acoustic power (solid black line) threads through a $\pm$50% swath that represents our estimate of the current ambiguity in extracting the numerical acoustic power from the simulation.

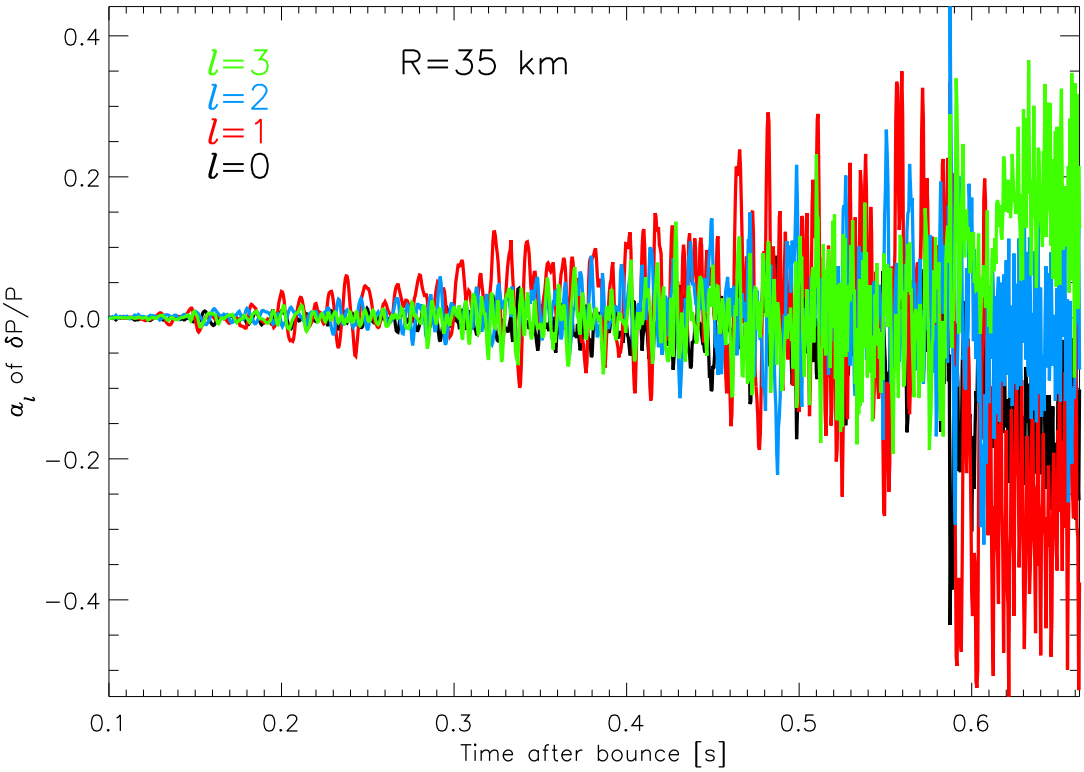

FIG. 7.— Time evolution of the spherical-harmonic coefficients for the fractional pressure variation for modes ℓ =0 (black), 1 (red), 2 (blue), and 3 (green) at a radius R = 35 km, given by $a_\ell = 2\pi \int_0^\pi d\theta \sin\theta Y_\ell^0(\theta)(P(R,\theta) - < P(R,\theta) >_\theta) / < P(R,\theta) >_\theta$. Notice that despite the fact that the ℓ =1 mode looms large, the ℓ =2 and ℓ =3 modes are also in evidence. The ℓ =2 (harmonic) mode will result in a distinctive signature in gravitational radiation detectors, initially at a frequency near ∼675 Hz. This frequency is likely to be different (higher) when general relativity is included (Ferrari et al. 2003).

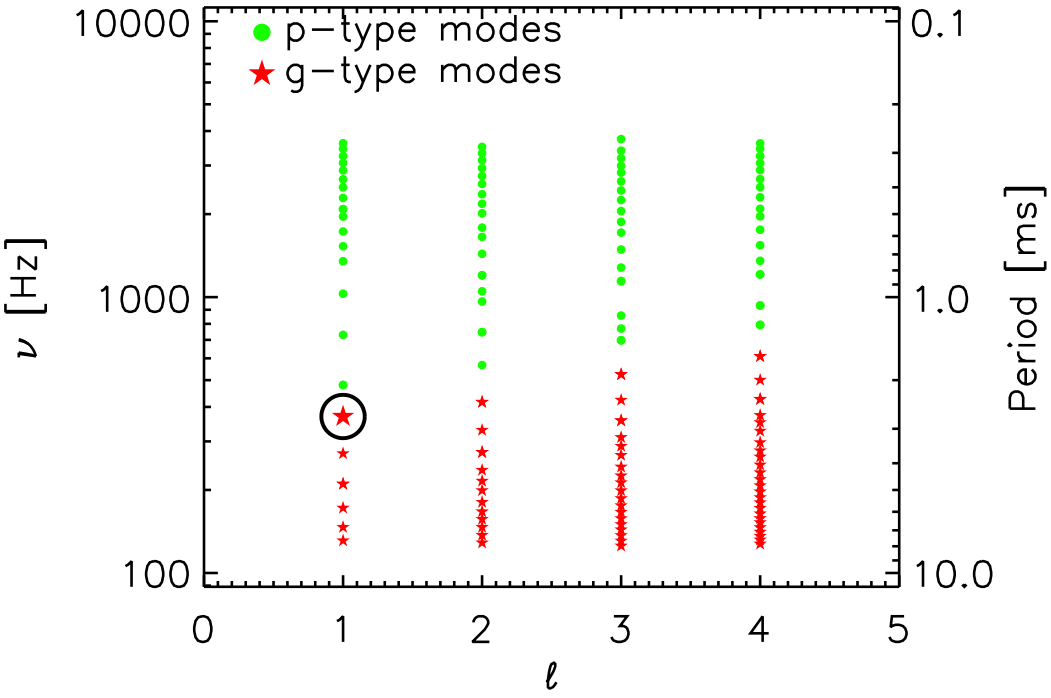

FIG. 8.— Frequency, ν, versus the index, ℓ, of the spherical-harmonic functions $Y_{\ell,0}(\theta,\phi)$ for the analytic core g-modes (red stars) and p-modes (green circles) obtained from a spherical average of the full 2D simulation profiles at 500 ms after bounce. The corresponding periods ($P = 1/\nu$) are given on the right axis. Nearly all modes have some g-type nodes and p-type nodes. The $\ell = 1$ mode highlighted with the circle corresponds to the mode with predominantly g-mode character which has been most easily excited in our simulation.

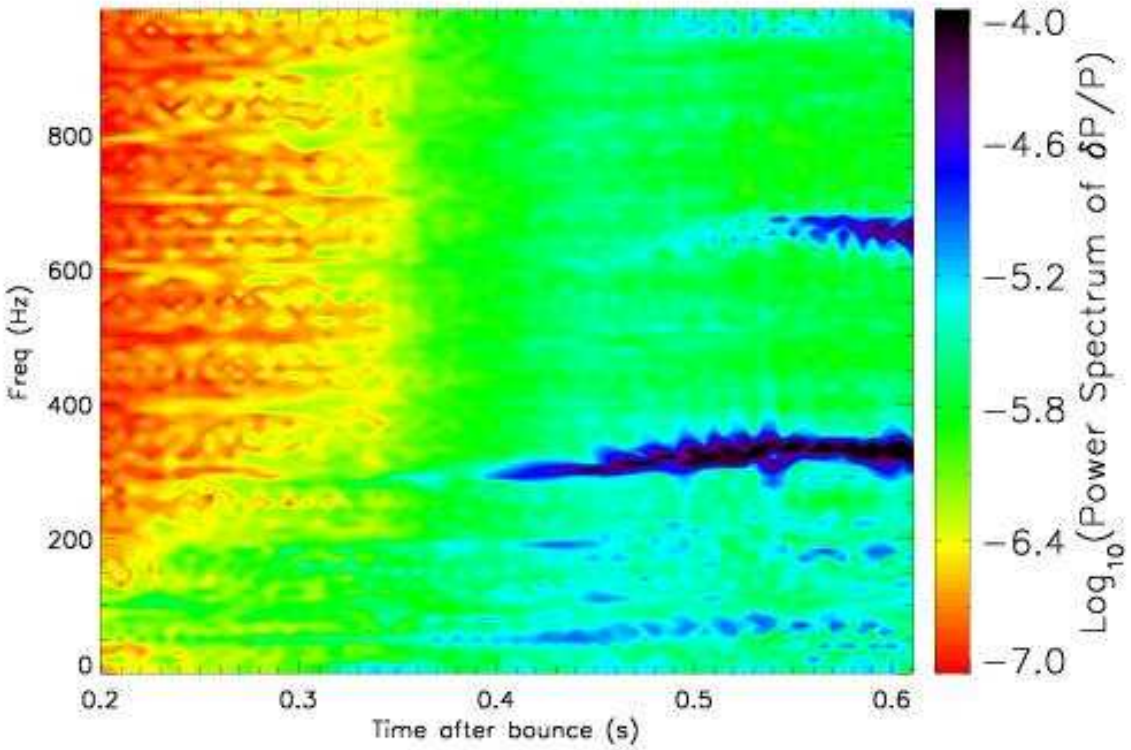

FIG. 9.— Colorscale of the power spectrum of the fractional pressure variation $(P(R,\theta) - < P(R,\theta) >_\theta) / < P(R,\theta) >_\theta$ at a radius $R = 30$ km, as a function of time and frequency. For each time t, a power spectrum is calculated from a sample of time snapshots covering $t \pm 50$ ms, at a resolution of 0.5 ms. Note the emergence of power in the ∼330 Hz ($\equiv 3$ ms) g-mode, as well as the strengthening $\ell = 2$ harmonic mode near ∼675 Hz at late times. The latter is of relevance for gravitational radiation emission.